Advances in Computer, Signals and Systems (2025)
Clausius Scientific Press, Canada

DOI: 10.23977/acss.2025.090119
ISSN 2371-8838 Vol. 9 Num. 1

Modeling and Simulation of E-Axles Electric Vehicle Based on Simulink

Hao Zhu[1], Xin Gu[2,3], Su Zhou[2,*]

[1]Shanghai Motor Vehicle Inspection Certification & Tech Innovation Center Co., Ltd, Shanghai, 201805, China
[2]Tongji University, Shanghai, 201804, China
[3]Shanghai New Power Automotive Technology Co., Ltd, Shanghai, 200438, China
[*]Corresponding author: suzhou@tongji.edu.cn

Keywords: Electric Vehicle; Electric Drive Axles; Analysis of Simulation; CHTC-TT

Abstract: Electrification of heavy-duty commercial vehicles represents a pivotal approach to addressing energy consumption and emissions. This study focuses on 49-ton heavy-duty commercial vehicles, employing electric drive axles to replace traditional engine propulsion systems. Research into the power performance and energy consumption of this system is conducted on this basis. As a fundamental method for analyzing these performance aspects, the establishment of models and performance simulations are indispensable steps in the development of electric systems. Effective modeling and simulation techniques can expedite the automotive development process and minimize costs. In this paper, a comprehensive plant model for E-Axle Electric Vehicle Systems is established, integrating various dynamics models. Utilizing the parameters of a 49-ton heavy-duty tractor, the economically optimal configuration for the E-axle is determined. Simulations based on the CHTC-TT cycle provide dynamic and economic indicators, facilitating comprehensive vehicle performance evaluations. Ultimately, the simulation results demonstrate that the E-axle system can meet the power performance requirements of the CHTC-TT cycle, achieving a maximum vehicle speed of 88 km/h over a 23 km journey while consuming 59 kWh of power. These findings indicate that the proposed configuration and matched parameters satisfy vehicle performance specifications, providing theoretical support for the electrification of heavy-duty commercial vehicles.

1. Introduction

With the rapid deterioration of air quality and the increasing scarcity of petroleum resources, significant advancements have been made in the research and development of new energy vehicles worldwide in recent years. Electric vehicles (EVs), serving as a transition from traditional engine vehicles to zero-emission electric vehicles, have become one of the main clean energy vehicles studied by countries, major automotive companies globally, as well as domestic scientific research institutions and universities[1]. Heavy-duty commercial vehicles account for less than 5% of the total vehicle ownership in China, yet they contribute to over 80% of carbon emissions and more than50% of fuel consumption[2]. Therefore, the electrification of heavy-duty commercial vehicles is of great

significance for energy conservation and emission reduction in the automotive sector. To meet the power requirements of these vehicles, 49-tonne heavy-duty commercial vehicles are typically equipped with two drive axles. To achieve the electrification of 49-tonne heavy-duty commercial vehicles, it is necessary to design these two drive axles as electric drive axles, which poses high demands on both the power performance and economy of electric heavy-duty commercial vehicles [3].To conduct preliminary research on the performance and fuel consumption of electric drive axles for heavy-duty vehicles, the best approach is to establish corresponding plant models. Currently, the development of electric commercial vehicles with electric drive axles based on model-based design has become the primary development method adopted by major automobile manufacturers worldwide. Among these, the establishment of models and performance simulation are crucial steps in the development of electric systems. Effective modeling and simulation can accelerate the automotive development process and reduce costs [4].This paper aims to establish a comprehensive Simulink plant model for a 49-ton heavy-duty semi-trailer, incorporating various key components and systems. By integrating models such as the vehicle's overall resistance model, Pacejka magic tire model, road conditions model, E-Axle, and Gearbox/differential model, a detailed simulation environment is created. The CHTC-TT driving cycle is employed to assess the vehicle's performance and fuel consumption, with a focus on evaluating the effects of retrofitting the semi-trailer with dual electric drive axles. The results provide insights into the energy efficiency and performance improvements achieved through this modification.

2. E-Axles Commercial Vehicle and Powertrain Structure

Figure 1 illustrates the overall architecture of a 49-tonne heavy-duty semi-trailer commercial vehicle. To meet the vehicle's dynamic performance requirements, it is equipped with two drive axles, which derive power from a single engine and always operate in unison for propulsion. However, following the transition to full electrification, the power layout for the dual electric drive axles of heavy-duty commercial vehicles becomes highly flexible, allowing for independent driving of each axle or combined driving of both. Given the wide power demand range of 49-tonne heavy-duty commercial vehicles, to avoid situations where the drive motors are either over-capacity or under-capacity for extended periods and considering the placement of drive motors and overall costs, this study designs a configuration with two drive motors for the dual electric drive axles of the heavy-duty commercial vehicle[5-6]. Specifically, one drive motor is installed on the front drive axle, and another on the rear drive axle, to further enhance the vehicle's dynamic performance.

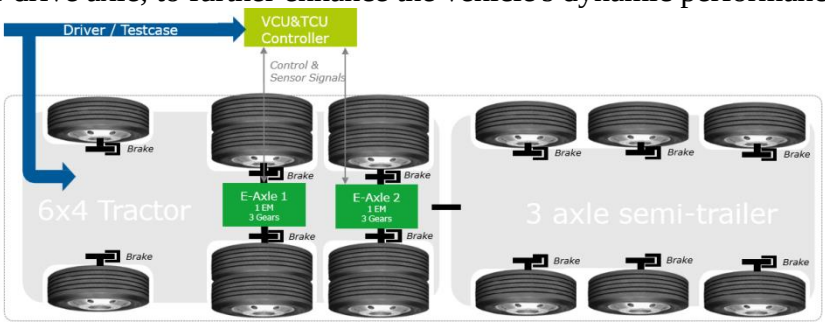

Figure 1 Overview of the vehicle & powertrain architecture with Controller

To fulfill the torque requirements of the 49-tonne heavy-duty commercial vehicle and reduce the demands placed on the drive motors, enabling them to operate more frequently within their high-efficiency ranges, transmission devices are incorporated into the dual electric drive axles. Currently, transmissions in electric drive axles primarily include single-speed, two-speed, and multi-speed options[7]. Taking into account the heavy-duty commercial vehicle's need to accommodate multiple

operating conditions and energy consumption concerns, two identical three-gears transmissions are designed for the front and rear axles, respectively. This transmission design effectively balances the vehicle's performance across various scenarios while optimizing energy efficiency[8].

3. Modeling of E-Axles Vehicle Systems

In order to simulate the overall vehicle performance of electric axle commercial vehicles, this paper establishes a Simulink plant model that incorporates various dynamic modules, including a longitudinal dynamics vehicle model, an E-axle model with a differential, tire and road models, a simplified brake model, a simplified shifting logic, E-motor efficiency characteristics, and a simple thermal derating logic. The full-vehicle simulation model platform for dual electric axles with a single motor per axle is illustrated in Figure 2. This model platform provides a comprehensive framework for analyzing and evaluating the performance of electric axle commercial vehicles under various driving conditions and operational scenarios. The plant model incorporates several input parameters, namely the E-axle gear ratio, the differential lock state, the brake pedal position, and the E-Motor demand torque. The outputs of this model encompass Vehicle parameters such as velocity, axle load, and wheel speeds, as well as E-motor characteristics including E-Motor speed, and the minimum and maximum torque values. This comprehensive model allows for a detailed analysis of the electric axle's performance and integration within the overall vehicle dynamics.

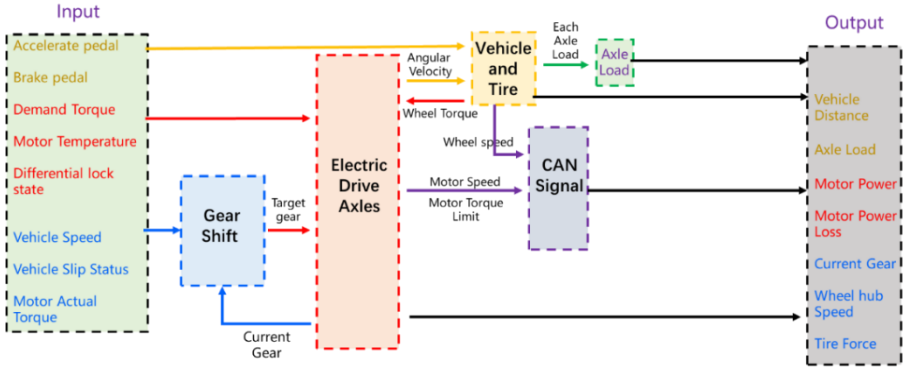

Figure 2 Concept Level Development Plant Model for Electric Axles Commercial Vehicle

3.1 Electric Drive Axles Model

The electric drive axle model is the core of modeling for E-Axles vehicle systems. Its function is to calculate the dynamic outputs of each wheel, the torque limit of the motor, and other relevant signals based on the provided current gear, motor torque, and torque of each wheel, then can calculate the angular acceleration of each axle.

As illustrated in Figure 3, the e-axle model is structured as follows:

1) E-motor Torque Model: This component simulates the torque output of the electric motor.

2) E-motor Efficiency Model and Simple derating logic: This module accounts for the efficiency of the electric motor and incorporates simple logic to adjust the motor's performance under various operating conditions.

3) Shift Process Logic: This represents the decision-making process for shifting gears, based on parameters such as vehicle speed, motor torque, and other relevant factors.

4) Gear Ratio and Efficiency Definition: This section defines the gear ratios and efficiencies associated with each gear in the transmission.

5) Gearbox Differential Model: This comprehensive model simulates the dynamic behavior of the gearbox and differential, including the inertias of the rotating components such as gears, shafts, and

differentials.

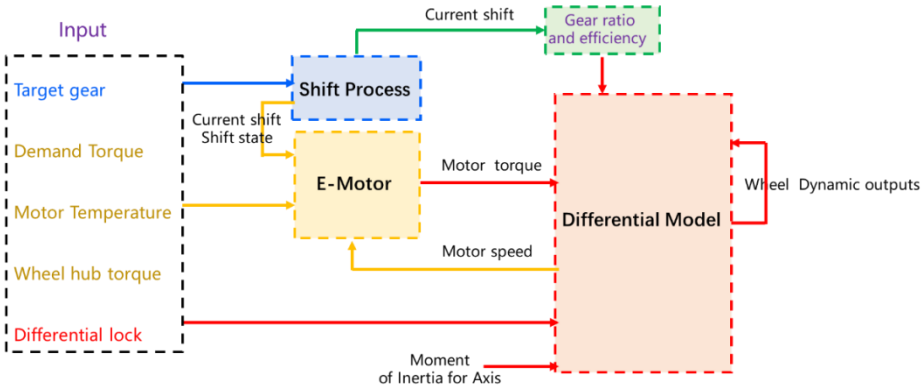

Figure 3 Plant Model Architecture for Electric Drive Axles

3.1.1 Shift Process Model

In this study, a straightforward shifting logic is implemented to ensure a reasonable shifting time for the e-axle within the vehicular powertrain system. Additionally, signals indicating the shift-in-process and driveline disengagement status are computed. The initiation of the shifting process is triggered by a new gear request from the Transmission Control Unit (TCU). A detailed explanation of the shifting process is provided in the subsequent section.

For the torque ramp-down and ramp-up phases, a typical time duration is calibrated to define the required period for reducing the torque from the reference value to zero or increasing it from zero to the reference torque. The shift process model plays a crucial role in the vehicular powertrain system, as it accurately calculates and determines the precise timings for gear shifting, speed regulation, neutralizing the transmission, and torque recovery based on predefined gear strategies. Furthermore, this model has capability to monitor and provide real-time feedback on vehicle's current gear status.

The shifting process is divided into the following phases for precise description as shown in Figure 4:

1) Pre-Shift Normal Driving: The driveline is engaged with the wheels, and there is no torque intervention by the TCU.

2) Torque Reduction Phase: The torque is gradually decreased from the demanded value to zero. This is achieved through the use of control mode 3, which is a limit control mode. During this phase, the driveline remains connected to the wheels.

3) Driveline Disengagement: The dog clutch is moved to the neutral position, effectively disconnecting the e-motor from the wheels. This results in the driveline being disengaged.

4) Speed Synchronization Phase : This phase, which involves synchronizing the speeds of the input and output shafts of the transmission, is not considered within the scope of the plant model in this context.

5) Driveline Engagement: The dog clutch is moved to the position corresponding to the intended gear selection, and the e-motor is reconnected to the wheels. This re-engages the driveline.

6) Torque Increase Phase: The torque is gradually increased from zero to the demanded value. This is also accomplished using control mode 3, the limit control mode. During this phase, the driveline remains connected to the wheels.

7) Post-Shift Normal Driving: The driveline remains engaged with the wheels, and there is no further torque intervention by the TCU, allowing for normal driving conditions to resume.

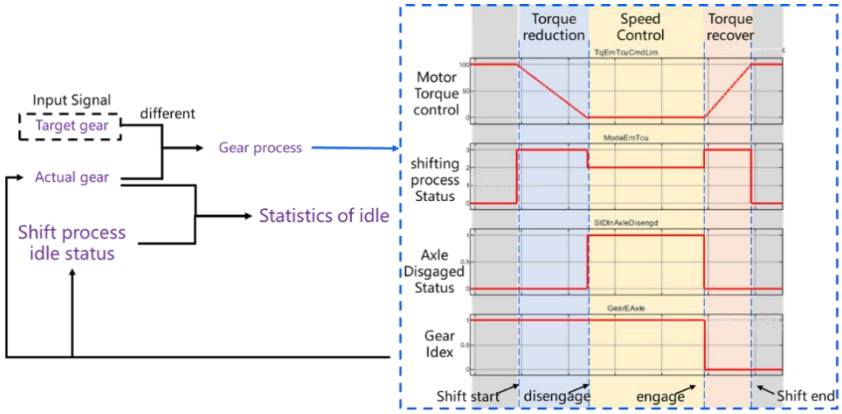

Figure 4 The logic diagram of the Shift Process Model

3.1.2 E-motor Model

The primary objective of the electric motor torque model is to accurately compute the torque output based on the motor's speed and the desired torque input. Within this framework, the desired torque is constrained by the maximum and minimum values feasible according to the inherent characteristics of the e-motor (Figure 5). To capture the dynamic behavior of the torque, the limited desired torque undergoes a delay and is subsequently filtered through a PT1 filter, which yields the final e- motor torque.

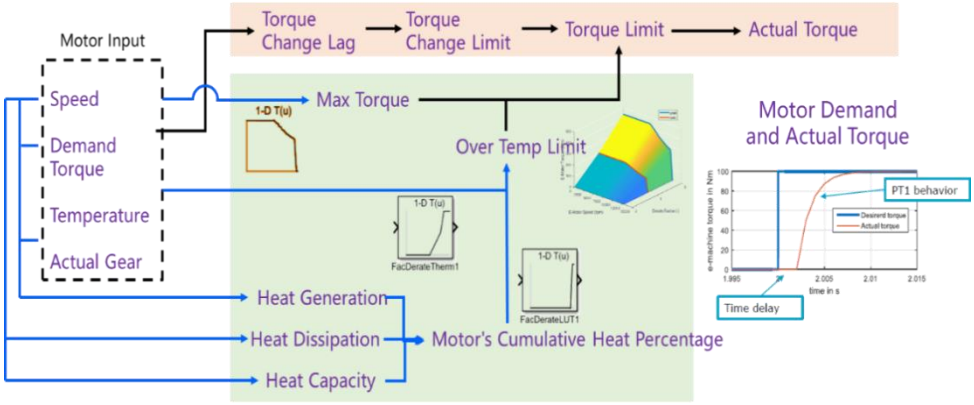

Figure 5 The logic diagram of Motor Model

A thermal model for electric motors has been implemented to facilitate both peak and continuous operational capabilities. The design of the e-motor's cooling system is typically tailored to ensure the complete and sustained dissipation of power losses incurred during full continuous operation. Consequently, the maximum cooling power performance is determined by the losses, which are calculated using an efficiency map and occur along the full continuous torque curve.

$$P_{el,cont} = \frac{P_{m,cont}}{\eta_{e,cont}} \tag{1}$$

$$P_{cool,Max} = P_{loss,cont} = P_{el,cont} - P_{m,cont} \tag{2}$$

When the continuous torque curve is exceeded, power losses typically increase further. The difference between these losses and those at the continuous torque curve corresponds to the heat power transferred to the mechanical components of the e-motor, such as the windings and housing, leading to an elevation in e-motor temperature.

$$P_{loss,act} = \frac{P_{m,act}}{\eta_{e,act}} - P_{m,act} \quad (3)$$

$$P_{heat} = P_{loss,act} - P_{cool,max} \quad (4)$$

Wherein $P_{el,cont}$ represents the continuous electrical power of the e-motor, while $P_{m,cont}$ denotes the continuous mechanical power. The efficiency at the continuous operating curve is indicated by $\eta_{e,cont}$. The maximum cooling power of the system is designated as $P_{cool,max}$. The design of the e-motor's cooling system is tailored to ensure the complete and sustained dissipation of $P_{loss,cont}$. When operating beyond the continuous torque curve, the power losses typically increase, necessitating a cooling system capable of handling $P_{cool,max}$ to prevent an elevation in e-motor temperature.

The maximum thermal capacity of the electric motor is derived from the maximum operation time t_{max} at the peak torque curve, prior to the necessity for derating. The maximum thermal energy $Q_{th,max}$ that can be accumulated in the mechanical components, before reaching the maximum temperature threshold and necessitating derating, is determined by the cumulative power losses at the peak torque curve, reduced by the maximum cooling power.

$$P_{heat,act} = P_{loss,peak} - P_{cool,max} \quad (5)$$

$$Q_{th,max} = \int_0^{t_{max}} P_{heat,max} \quad (6)$$

This energy storage capacity is maintained until the e-motor derating mechanism is activated. The instantaneous thermal energy of the e-motor Q_{th} is computed using a specific formula

$$Q_{th} = \int_0^t P_{heat} \quad (7)$$

where the thermal energy generally correlates with the e-motor temperature. However, calculating the e-motor temperature is challenging due to the unknown thermal mass and the distribution of thermal energy into various parts with differing, unknown heat transfer coefficients. Consequently, explicit temperature calculation is not performed, as it is not pertinent to the derating approach. Instead, the current thermal energy is compared to the maximum thermal energy for the purpose of derating. When the maximum thermal energy of the electric motor (e-motor) is surpassed, peak load operation becomes infeasible, triggering the activation of e-motor derating. This derating process involves reducing the maximum torque to the level of the continuous torque curve ($Q_{th} > Q_{th,max}$), thereby implementing torque limitation to the continuous torque curve. This limitation is executed through a derating factor and a torque limit map. As the normalized thermal energy ($Q_{th,max}$) approaches a value of 1, the derating factor increases from 0 to 1 (or even to 2) using a ramp function. A derating factor of 2 signifies that the e-motor is unable to apply any torque. Conversely, when the e-motor operates below the continuous torque curve, the heat power (P_{heat}) becomes negative, leading to an automatic decrease in thermal energy. This indicates sufficient cooling power to dissipate the current losses and further reduce the thermal energy of the e-motor's mechanical components. Consequently, peak operation becomes feasible once again ($Q_{th} < Q_{th,max}$), allowing the e-motor to resume peak operation.

3.1.3 Gearbox Differential Model Model

The equations of motion for the mechanical e-axle paths are solved using inputs such as e-motor torque, gear ratio, differential lock state, and left/right wheel hub torques (Figure 6). In this context, the gear ratio and the differential lock state are defined as constants over the entire simulation period.

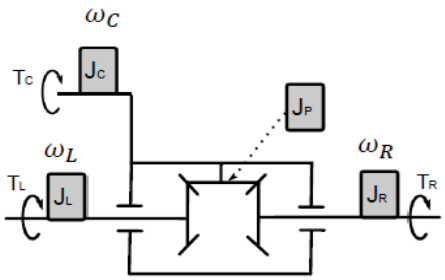

Figure 6 The mechanical structure of the differential

The inertia components considered in the equations include the E-Motor inertia, the inertia of the e-axle gearbox parts, the differential cage parts (denoted as J_{diff}), the inertia of the differential left-side part and left-side wheel (denoted as J_{Lt}), and the inertia of the differential right-side part and right-side wheel (denoted as J_{Rt}). The differential torque (T_c) is determined based on the E-Motor torque, transmission ratio, and efficiency. The wheel hub torques acting on the left (T_{L}) and right (T_{R}) sides of the differential are considered as negative values of the respective wheel hub torques (T_{HubL} and T_{HubR}). Additionally, the left and right wheel speeds (ω_{L} and ω_{R}) and differential speed (ω_{C}) are calculated. The gear ratio of the planet gear versus the axle side bevel gears (L or R) is denoted as i_p, and the number of planet gears is represented by n_p.

By solving using Lagrange's equations, we can obtain:

When the differential lock is engaged, the result is denoted as,

$$(J_{Diff} + J_{Rt} + J_{Lt})\dot{\omega}_C = T_C + T_R + T_L \tag{8}$$

When the differential lock is not engaged, the result is denoted as,

$$\begin{bmatrix} J_{Rt} + J_{Lt} + n_p J_p {i_p}^2 & -2J_{Lt} - n_p J_p {i_p}^2 \\ -2J_{Lt} - n_p J_p {i_p}^2 & J_{Diff} + 4J_{Lt} + n_p J_p {i_p}^2 \end{bmatrix} \begin{bmatrix} \dot{\omega}_R \\ \dot{\omega}_C \end{bmatrix} = \begin{bmatrix} T_R - T_L \\ T_C + 2T_L \end{bmatrix} \tag{9}$$

This allows to solve for the angular acceleration of each shaft in the gear differential based on torque.

3.2 Vehicle and Tire Model

The architecture of the vehicle and tire model, as illustrated in Figure 7, is designed to compute various parameters and variables, including wheel torque, axle load, and vehicle speed, based on the input signals from the brake pedal and wheel angular velocity.

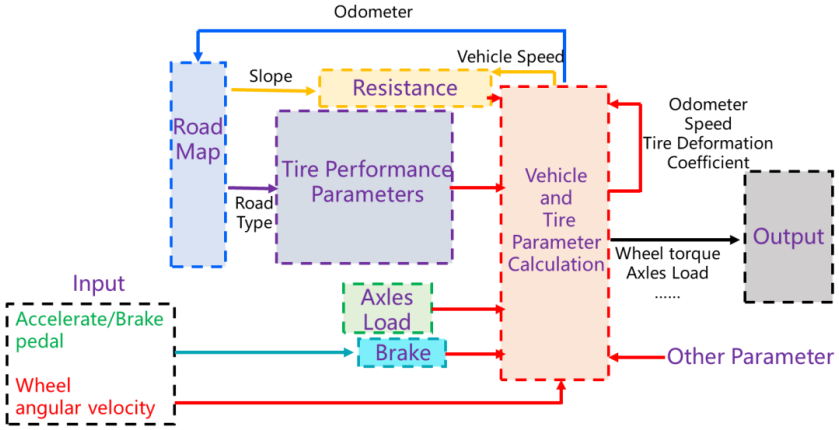

Figure 7 The structure of the Vehicle and Tire Model

3.3.1 Brake and Resistance Force

The role of vehicle dynamics modeling is to compute the overall driving force and resistance torque of vehicle. In this paper, the lateral and vertical dynamic characteristics were neglected when modeling the vehicle's motion equations, focusing solely on the establishment of a longitudinal dynamics model. By determining the longitudinal dynamics model, the motion status of the vehicle along its travel direction is established. Therefore, it is crucial to understand the various external forces acting on the vehicle in the direction of travel, namely the driving force and the driving resistance. The vehicle's motion equation, derived from the balance of these forces, constitutes the longitudinal dynamics model of the vehicle. [9]

$$F_{Brk} = k_{ped} f_{brk} m_{veh} g \tag{10}$$

$$F_{Res} = F_{drag} + F_{roll} + F_{drag} + F_{grad} = \frac{\rho_{air} C_w A_{veh}}{2} V_{veh}^2 m_{veh} g cos(\alpha) C_\gamma + m_{veh} g sin(\alpha) \tag{11}$$

3.3.2 Pacejka magic tire model

The Pacejka magic tire model is employed to compute the torque of each wheel and various vehicle operational parameters through a systematic method (Figure 8). Initially, a single-contact-point transient model is utilized to equate the forces induced by tire deformation to the restorative forces resulting from spring elongation, thereby facilitating the calculation of tire slip rates. Subsequently, based on the transient tire slip, tire forces are derived using the magic formula methodology. Ultimately, the longitudinal vehicle dynamics are assessed utilizing the vehicle equation of motion[10].

Step1: Tire transient slip calculation:

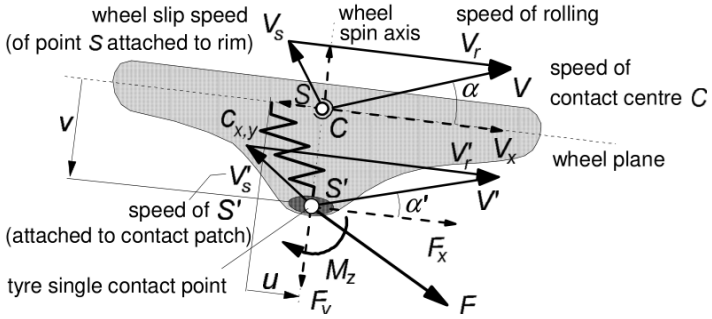

Figure 8 The mechanism of Pacejka magic formula tyre model [10]

(a) Calculate the Slip velocity based on vehicle speed, wheel angular velocity, and wheel radius

$$v_{slip} = v_{veh} - r_w \omega_w \tag{12}$$

Wherein v_{slip} denotes slip velocity, v_{veh} denotes vehicle speed, r_w means wheel radius and ω_w is wheel angular velocity.

(b) Based on slip stiffness and longitudinal tire stiffness, relaxation length is calculated

$$\sigma_K = C_{F\kappa}/C_x \tag{13}$$

Wherein σ_K denotes relaxation length, $C_{F\kappa}$ denotes slip stiffness, C_x means longitudinal tire stiffness.

(c) Based on the slip velocity and the relaxation length, the time derivative of the longitudinal carcass deflection is calculated

$$\dot{u} = -v_{slip} + v_{slip}' = -v_{slip} - |v_{veh}|u/\sigma_K \tag{14}$$

Wherein u denotes longitudinal carcass deflection, v_{slip} denotes slip velocity, σ_K denotes

relaxation length.

(d) The transient slip is calculated based on the longitudinal carcass deflection and the relaxation length. For low velocities, an additional damping term proportional to v_{slip} must be included because of numerical stability.

$$\kappa' = u/\sigma_K - v_{slip} k_{vlow}(v_{veh})/C_{F\kappa} \tag{15}$$

Wherein κ' denotes transient slip.

(e) At last, the transient tire slip is calculated based on the transient slip.

$$\sigma = \kappa'/(1+\kappa') \tag{16}$$

Wherein σ denotes transient tire slip.

Step 2: Tire force calculation:

Based on the transient tire slip σ tire forces are calculated using a magic formula approach.

$$F_{xi} = D_{xi}\sin(C_{xi}\text{atan}(B_{x,i}\sigma_i - E_{xi}(B_{x,i}\sigma_i - \text{atan}(B_{x,i}\sigma_i)))) \tag{17}$$

The Magic Formula coefficients $B_{x,i}$, C_{xi}, D_{xi}, E_{xi} are define as follows.

■ A wheel load dependent friction coefficient $\mu_{x,i}$ is used. $\mu_{x,0}$, $k_{\mu,x}$ and F_{z0} are tire parameters. With the friction coefficient the MF parameter D_{xi} can be calculated

$$\mu_{x,i} = \mu_{x,0}(1 + k_{\mu,x}(F_{z,i} - F_{z0})/F_{z0}) \tag{18}$$

$$D_{xi} = F_{z,i}\mu_{x,i} \tag{19}$$

■ The MF Parameters B_{xi} are calculated based on the tire parameters K_x and C_x and the friction coefficient $\mu_{x,i}$.

$$B_{xi} = K_x/(C_x\mu_{x,i}) \tag{20}$$

Wherein i indicates the tire index $i \in [L1, R1, L2, R2]$.

To simulate the behavior of traction control across a spectrum of friction conditions, the paper have implemented eight distinct tire parameter sets (Table 1), each representing a unique friction scenario ranging from 1 to 8. These scenarios encompass a variety of terrains and tire conditions, including dry, wet, snowy, icy surfaces, as well as off-road terrains. Additionally, the study have incorporated different tire wear statuses to reflect the practical realities of tire degradation. Depending on the friction condition, the optimal slip ratio may vary significantly, ranging from approximately 1.8% to 100%. Notably, during challenging off-road driving conditions, a high slip ratio of 100% may be advantageous for achieving high longitudinal force transfer. For the implementation of tire-road friction conditions in plant model, the study have defined a distance-dependent look-up table for each of the four driven tires. This approach allows for the easy simulation of varying friction conditions.

Table 1 Summarizing Vehicle tire Parameters

No	Description	$\mu_{x,0}$ [-]	$k_{\mu,x}$ [-]	F_{z0} [N]	K_x [-]	C_x [-]	E_x [-]
1	dry paved road - wear state1	1	-0.08	49050	10.00	1.4601	-3.612
2	wet paved road - wear state1	0.6	-0.08	49050	10.00	1.4601	-0.209
3	dirt off-road surface	0.6	-0.08	49050	10.00	1.0901	0.862
4	extreme off-road curve	0.6	-0.08	49050	1.00	1.0901	0.951
5	dry paved road - wear state2	1	-0.08	49050	17.79	1.56	-0.609
6	wet paved road - wear state2	0.7	-0.08	49050	17.79	1.56	-0.609
7	snow raod	0.4	-0.08	49050	17.79	1.56	-0.609
8	ice road	0.15	-0.08	49050	17.79	1.56	-0.609

Step 3: Vehicle acceleration calculation:

Based on vehicle equation of motion (longitudinal), the paper calculate the vehicle speed, acceleration speed and wheel hub torques.

$$\dot{v}_{veh} = \frac{F_{xL1}+F_{xR1}+F_{xL2}+F_{xR2}-F_{res}}{m_{veh}+\mathrm{n}J_w\frac{1}{r_w{}^2}} \tag{21}$$

Where m_{veh} indicates vehicle mass, J_w denotes wheel inertia and n means non drive wheel number.

4. Simulation of E-Axle Electric Vehicle Systems

After completing the modeling of Electric Axles Commercial Vehicle, the calibration of the plant model is subsequently carried out based on the predefined parameters of the entire vehicle and its powertrain system. Furthermore, a standardized driving cycle is employed to conduct simulation validation of the model. This validation process aims to verify whether the vehicle's critical dynamic performance indicators, such as vehicle speed, gear shifting, and driving torque, as well as its economic indicators, including electricity consumption and equivalent fuel consumption, meet the operational requirements. Through this comprehensive approach, we ensure that the modeled electric axles for commercial vehicles not only exhibit the desired dynamic characteristics but also achieve satisfactory economic performance in simulated driving scenarios.

4.1 Overview of Vehicle and Powertrain main parameters

The paper employs a mature 49-tonne heavy-duty commercial vehicle available in the market as the prototype for modification, with its complete vehicle parameters shown in Table 2.

Table 2 Summarizing Vehicle Parameters

Vehicle	**Unit**	**Value**
Vehicle type	-	Semi-Trailer Truck
Vehicle weight truck	tons	9.94
Vehicle weight truck w/ empty trailer	tons	20.5
Vehicle weight truck w/ fully loaded trailer	tons	48.958
Axle configuration Truck	-	6x4
Axle Load Distribution truck only	kg	5360/2620/1960
Axle Load Distribution truck w/empty trailer	kg	5840/4740/4900/5400/2240/3400
Axle Load Distribution truck w/ fully loaded trailer	kg	6532/8922/8922/8194/8194/8194
Frontal area	$_m$2	9.0
Drag coefficient	-	0.7
Tire type	-	12R22.5 18PR tubeless radial tires+22.5×9.0 wheels
Tire inertia	kgm ²	15
Dynamic rolling radius	m	0.527
Rolling resistance coefficient	-	0.0065
Rolling resistance coefficient zero Order	-	0.00493
Rolling resistance coefficient first Order	h/km	4.35E-05

After the modification, the powertrain adopted two identical three-gear electric drive axle systems, with its parameters listed in Table 3.

Table 3 Summarizing Powertrain Parameters

E-Axle QE350 (identical for both e-axles)	Unit	Value
Number of identical e-motors (per e-axle)	-	1
E-motor power (per e-motor) (cont./peak)	kW	160 / 320
E-motor torque (per e-motor) (cont./peak)	Nm	200 / 440
E-motor Peak time	s	30
Number of gears (per e-axle)	-	3+N (1/2/3/N)
Ratio gear 1	-	87.37052
Ratio gear 2	-	40.220658
Ratio gear 3	-	19.66011
Mech. Efficiency gear 1 **	%	95.263
Mech. Efficiency gear 2 **	%	95.546
Mech. Efficiency gear 3 **	%	95.938

Figure 9 displays the efficiency of the electric drive axle system, which is a combination of inverter

efficiency and motor and transmission 3 gear efficiency. These efficiency are used to calculate the subsequent economic performance of the vehicle's powertrain.

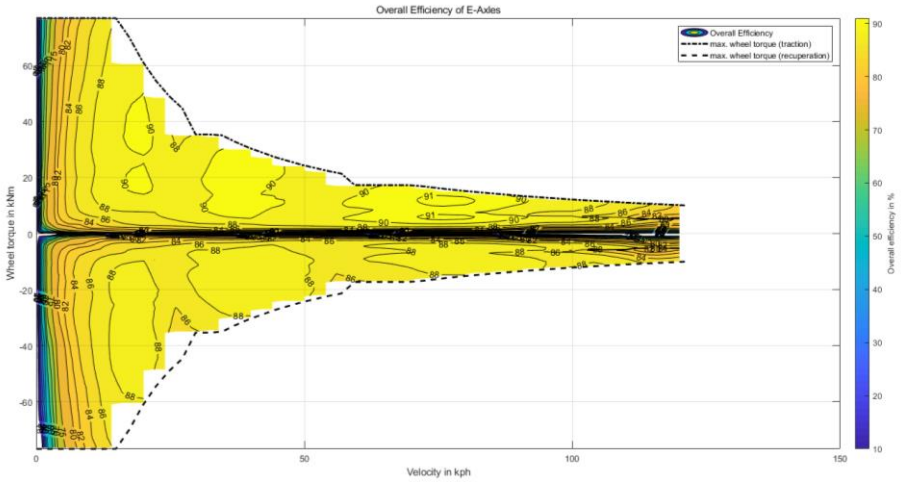

Figure 9 Overall. Efficiency of E-Axles

4.2 Simulation results and discussion

After establishing the plant model for E-Axle Electric Vehicle Systems and configuring the main parameters for the Vehicle and Powertrain, this paper employed the CHTC-TT cycle to conduct simulation validation of the constructed models. The objective was to ensure that the simulation results of the established vehicle resistance model, Electric Drive Axles Model, and Pacejka magic tire model adhered to physical laws and met the anticipated requirements. Ultimately, to investigate the potential energy consumption reduction associated with the adoption of Electric Drive Axles compared to conventional engines, a generalized energy management strategy was utilized. This strategy followed the velocity profile prescribed by the CHTC-TT, maintaining a 50:50% torque distribution to Em1 and Em2 at all times (excluding gearshifts). The total electrical energy consumed by two motors was assessed, and vehicle's dynamic performance was verified to meet the required velocity profile (ensuring that the actual vehicle speed could keep pace with the demanded speed). It is important to note that losses during recovered energy storage (HVB charging) and HVB discharging were not considered, nor were auxiliary losses taken into account in this analysis.

Figure 10 presents the comprehensive results obtained from physical model of vehicle during CHTC-TT cycle. Specifically, it displays the total mileage calculated, the vehicle speed, actual rotational speeds of the two electric motors, the wheel speeds of the front, middle, and rear wheels, as well as the driving and generate torques of the two motors. These data collectively provide insights into the performance characteristics of the vehicle during the simulated driving cycle. Figure 11 presents the simulation results of the Electric Drive Axles Model, which, in addition to showcasing demanded and actual torques of E-motor 1 and 2 along with their respective maximum and minimum torque limits, also displays left and right wheel speeds and differential speed within the Gearbox Differential Model. Furthermore, analysis delves into rotational speed deviations between left and right wheels relative to differential, providing insights into dynamic behavior of the axle system.

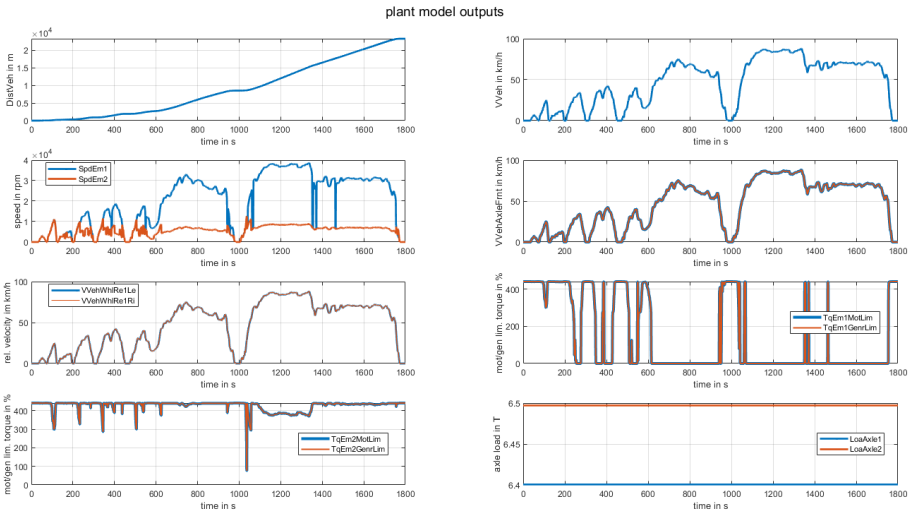

Figure 10 The output of vehicle and tire plant model

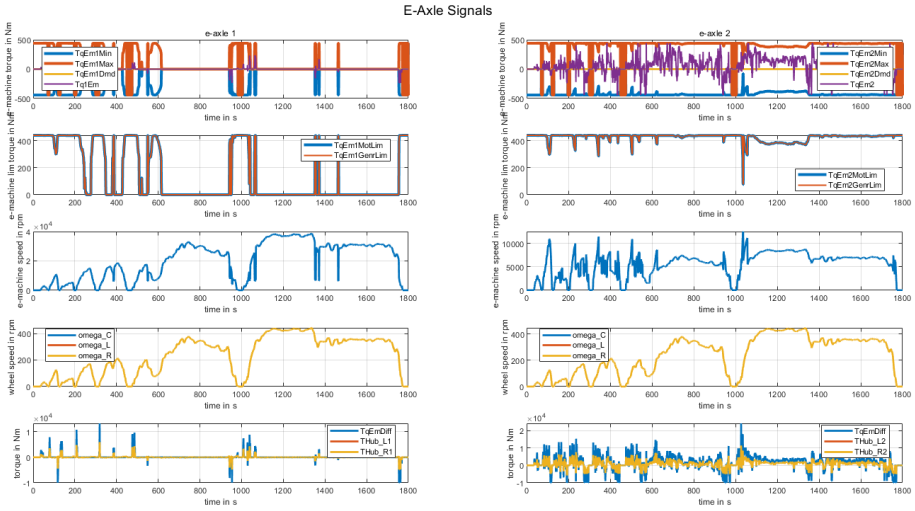

Figure 11 The output of Electric Drive Axles Model

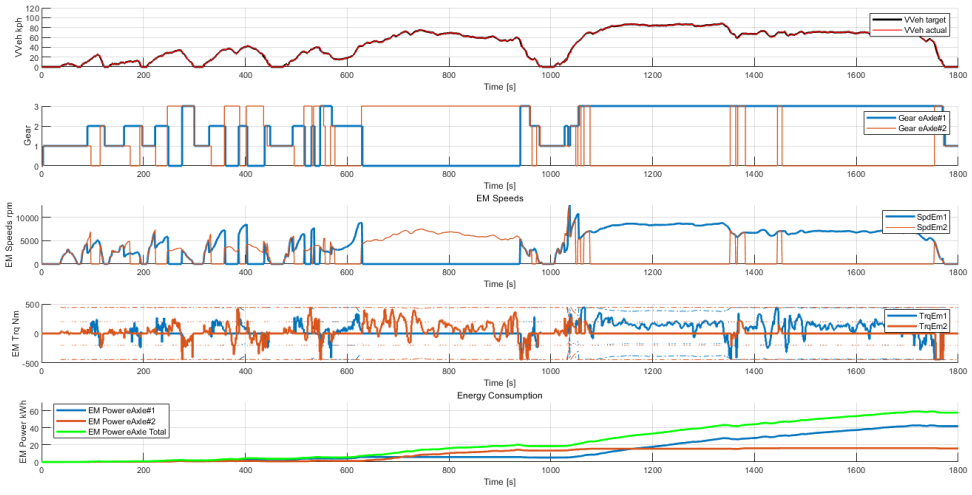

Figure 12 Energy Consumption of Electric Drive Axles

This paper conducted simulation validation on the dynamic performance and economy of CHTC-

TT driving cycle. The simulation results, presented in Figure 10, demonstrate that the actual vehicle speed could effectively keep pace with the demanded speed, thereby fulfilling the dynamic performance requirements. Furthermore, under the complete CHTC-TT driving cycle, the vehicle consumed 59 kWh of electrical energy, as illustrated in Figure 12. Additionally, the analysis encompasses the gear shifting patterns and the rotational speeds and torques of the two motors in the electric drive axle.

5. Conclusion

In this paper, a comprehensive plant model for E-Axle Electric Vehicle Systems is established, incorporating the magic formula tire model, the longitudinal dynamics vehicle model, the E-axle model equipped with a differential, as well as the vehicle and road models. Subsequently, based on established heavy-duty tractor products in the market, the parameters of vehicle and its powertrain system are determined, and the economic configuration of the E-axle is completed. Utilizing the constructed physical model, simulations are conducted using the CHTC-TT driving cycle, yielding dynamic and economic performance indicators. These results provide an improved simulation environment for subsequent performance simulations and evaluation of the vehicle improvement.

References

[1] BAI Yuhe, FAN Jianwen. TAN Guangxin. Modeling and Simulation of Parallel-Series Hybrid Electric Vehicle Based on Matlab ／Simulink[J]. JiSuanji Yu XianDaiHua 2014, 24-30

[2] Wang Yiting. Research on Driving Style Economy Prediction Model and Method Based on Big Data from the Internet of Vehicles [D]. Chang'an University, Shaanxi, 2023.

[3] Liu Benyou, Liu Junlong,Ji Jianyi, et al. Study on the Configuration Scheme Design and Parameter Matching of Heavy Duty Commercial Vehicles with Dual Electrical Drive Axle[J] Journal of Mechanical Transmission 2024,48(7):150-157

[4] Ma Jingzhan, Zuo Shuguang, He Zhisheng. Modeling and Simulation of Four-Wheel Drive Hybrid Electric Vehicles Based on Matlab/Simulink Environment [J]. Shanghai Auto, 2005(11):3. DOI: 10.3969/j.issn.1007-4554.2005.11.007.

[5] WANGZ Z,ZHOU J,RIZZONI G.A Review off Architectures and Control-strategies of Dual-motor Coupling Powertrain Systems for Battery Electric Vehicle[J].Renewable and Sustainable Energy Reviews.2022,162:112455.

[6] HUANG Jianfei, WANG Jianhua, JIN Di, et a1. Research Review of Electric Drive Axle[J]. Journal of Mechanical Transmission, 2020,44(11): 171- 176.

[7] Xu Xiangyang, Zhao Junwei, Dong Peng, et al. Technical characteristics and prospects of power transmissions for commercial vehicles under the Carbon-Peak and Carbon-Neutrality target [J]. J Automotive Safety and Energy, 2023, 14(4): 395-412.

[8] Wang Xiaojun, Cai Yuanchun, Zhou Yunshan, et al. A Study on the Effects of the Matching of Automatic Transmission on the Energy Consumption of Electric Vehicle [J]. Automotive Engineering, 2014(7): 871-878.

[9] Su Zhou. Modeling and Simulation Technology of Fuel Cell Vehicle, BeiJing Institute of Technology Press, ISBN 978 -7- 5682- 0362-3, 2017.1

[10] Hans B. Pacejka, Tyre and Vehicle Dynamics, 2006, Butterworth Heinemann/ Elsevier, UK